Published in final edited form as:
Ultrastruct Pathol. 2014 October ; 38(5): 335–343. doi:10.3109/01913123.2014.927406.

Implications of DNA Leakage in Eyes of Mutant Mice

Alexander J. Ogilvy, BS[1], **Defen Shen, PhD**[1], **Yujuan Wang, MD, PhD**[2], **Chi-Chao Chan, MD**[1], and **Mones S. Abu-Asab, PhD**[1]

[1]Laboratory of Immunology, National Eye Institute, Bethesda, MA, USA

[2]Sun Yat-sen University, Zhongshan Ophthalmic Center, Guangzhou, China

Abstract

Extranuclear DNA (enDNA) is not well studied ultrastructurally in the retinal pigment epithelium (RPE). We analyzed the retina and *vastus medialis* muscle of four mouse strains that are related to focal retinal degeneration by transmission electron microscopy (TEM) and EM immunolabeling. Evaluation of enDNA would imply the involvements of enDNA is either limited to the affected tissue or generalized in the whole body. Ultrastructural analysis and EM immunolabeling revealed that enDNA was present in the RPE cells but not in the muscle. These data suggest that enDNA could be unique to unhealthy RPE and a potential biomarker for cellular abnormality.

Keywords

Autophagy; enDNA; extranuclear DNA; hypoxia; mitochondria; retinal pigment epithelium; RPE; *vastus medialis*

Nuclear DNA leakage refers to extranuclear DNA (enDNA) or cytoplasmic DNA. The appearance of extranuclear chromatin elements in the cytoplasm is an understudied phenomenon; however, several studies described isolated elements from in vitro cultured cells and have not attempted to describe these elements in the in vivo native tissues [1–3]. Our observation of extranuclear chromatin in the cytoplasm in clinical cases has prompted us to question the frequency of enDNA (Figure 1) as well as its implications on cell pathology and survival.

Nuclear DNA leakage into the cytoplasm can be a catastrophic event for the cell with possible inflammatory consequences for the organism [4]. However, little is known about the triggers of this phenomenon, as well as its significance and downstream effects. Thus far, it is unclear whether enDNA is a sign of cell senescence or a pathological state. There are no evidences of an association between age-related macular degeneration (AMD) and enDNA, or an association between enDNA and abnormalities of cellular organelles such as mitochondria and melanosomes in the literature.

Correspondence: Dr. Mones S. Abu-Asab, PhD, Laboratory of Immunopathology, National Eye Institute/NIH, 9000 Rockville Pike, Bethesda, MA 20892, USA. mones@mail.nih.gov.

DECLARATION OF INTEREST

The authors declare no conflicts of interests. The authors alone are responsible for the content and writing of this article.

We have generated *Ccl2*$^{-/-}$/*Cx3cr1*$^{-/--}$mice from breeding *Ccl2*$^{-/--}$and *Cx3cr1*$^{-/--}$mice, both on C57BL/6N background [5]. The *Ccl2*$^{-/-}$/*Cx3cr1*$^{-/-}$ mice spontaneously develop elevated A2E and focal photoreceptor and retinal pigment epithelium (RPE) degenerations that mimic AMD. The C57BL/6N mouse has *Crb1*^{rd8} mutation, which could develop retinal dystrophy and dysplasia [6]. In contrast, C57BL/6J mouse does not have *Crb1*^{rd8} mutation and the morphology of the retina is normal [7].

Throughout our experiments, we sought to ultra-structurally examine and characterize enDNA, determine their association with transformations within other subcellular components such as mitochondria and melanosomes, the appearance of pathologic aberrations such as cytoplasmic degradation and excessive autophagy, and whether enDNA exists in both abnormal and normal tissues of our genetically engineered mice with progressive focal retinal degeneration.

MATERIALS AND METHODS

Mice

Four mouse strains were studied ultrastructurally and with immunolabeling electron microscopy. The wild-type negative control was the C57BL/6J, and the positive control was the C57BL/6N strain. Two mutant mice strains with C57BL/6N background: the *Ccl2*$^{-/-}$ and double knockout *Ccl2*$^{-/-}$/*Cx3cr1*$^{-/-}$. A total of 24 mice were used, 6 from each strain. All mice were between 1 to 6 months old. Prior to eyes enucleation, a fundoscopy was performed to provide the presence of retinal lesions. All animal experiments were performed under protocols approved by the NEI's Institutional Animal Care and Use Committee and were in compliance with the Association for Research in Vision and Ophthalmology Statement for the Use of Animals in Ophthalmic and Vision Research.

Transmission electron microscopy (TEM)

Mouse eyes were enucleated and *vastus medialis* muscles were harvested immediately after death. The eyes and muscles were doubly-fixed in PBS-buffered glutaraldehyde (2.5% at pH 7.4) and PBS-buffered osmium tetroxide (0.5%), and embedded in epoxy resin. Thin sections (90 nm) were collected on 200-mesh copper grids, dried for 24 h, and double stained with uranyl acetate and lead citrate. Sections were viewed and photographed with JEOL JM-1010 electron microscope.

Immuno TEM

Mouse eyes prepared for immunolabeling were fixed in 4% formalin and embedded in LR White acrylic resin (SPI, West Chester, PA). Thin sections (150 nm) were collected on 200-mesh nickel grids, dried for 24 h, and washed with a 1:1 dilution of blocker and PBS for 20 min (PBS, 0.1% Tween 20, 0.5% cold-water fish gelatin [Ted Pella, Inc., Redding, CA]), then a 1:50 dilution of rabbit anti-mouse histone H3 antibody (Abcam, Cambridge, UK; http://www.abcam.com/) in blocker solution for 1 h, washed in the blocker dilution once, soaked in a 1:100 dilution of gold-conjugated protein A (Sigma, St. Louis, MO; http://www.sigmaaldrich.com) in blocker, then washed once in PBS and once in deionized water, then air-dried. Immunolabeled grids were stained with aqueous uranyl acetate (5%). In TEM

micrographs, secondary gold-conjugated antibodies appear as small black dots with well-defined edges.

RESULTS

Baseline fundoscopy showed focal retinal lesions in the three mouse strains with C57BL/6N background (*Crb1*^{rd8} mutation), but not in C57BL/6J (normal *Crb1*) mice (Figure 2). The retinal lesions were much more severe in the *Ccl2*$^{-/-}$and *Ccl2*$^{-/-}$/*Cx3cr1*$^{-/-}$ strains than in C57BL/6N.

In mice with C57BL/6N background (*Crb1*^{rd8} mutation), enDNA leaks were abundant and severe (Figures 3B–D and 4B–D), however, they only occurred when the RPE cells appeared unhealthy having cytoplasmic vacuoles, excessive glycogen, degenerate melanosomes, and disorganization of mitochondria and melanosomes. Lesions of enDNA were confirmed by immunolabeling (Figure 4). The presence of enDNA was often associated with abnormal mitochondria (Figure 5B–D), deteriorating chromatin, and/or nuclear membrane (Figure 3B–D). Those RPE cells with enDNA lacked signs of apoptosis and damaged nuclei, indicating that such DNA leakage might not be due to programmed cell death.

The C57BL/6J mouse was without ultrastructural lesions in the retina. In the RPE, enDNA was not observed (Figure 3A), the cytoplasm was normal, with few lipid droplets, and glycogen, and occasional vacuoles (Figure 5A). The nuclear envelope, composed of the outer and inner nuclear membranes, nuclear lamina and nuclear pore complexes is well-defined, with no observable breaches (Figure 3A). The mitochondria were located basally and possessed well-defined cristae (Figure 5A). Furthermore, the mitochondria showed no signs of autophagy and degeneration. Melanosomes were healthy and arranged toward the apical side of the cell. Immunolabeling of H3 histone protein showed no enDNA (Figure 4A).

Few lesions could be present in the deep retina of some C57BL/6N mice (Figure 2B). In the RPE, enDNA was identified (Figure 3B). The cytoplasm was abnormal, with irregular densities and many vacuoles and few lipid droplets (Figure 3B). Degradation of the cytoplasm appeared around the nucleus and melanosomes. The nuclear envelope lacked clear structure, and pyknotic chromatin material could be observed protruding from the nucleus. Mitochondria also appeared abnormal, with poor definition of their cristae (Figure 5B). Some mitochondria even lacked any definition, appearing as blobs with high electron density. Melanosomes were arranged apically and appeared shriveled and were not infiltrated by resin. Immunolabeling of H3 histone protein was positive within the nucleus and in the cytoplasm near the nucleus (Figure 4B).

The *Ccl2*$^{-/-}$ knockout mutant had many abnormalities in the retina. Many enDNA were observed (Figures 3C and 4C). In the RPE, the cytoplasm was abnormal, containing large lipid droplets, numerous vacuoles, and significant amounts of glycogen (Figure 5C). Pyknotic chromatin material was seen in clusters adjacent to the ill-defined nuclear envelope (Figure 3C). Mitochondria had poorly defined cristae (Figure 5C), some of them appeared to

be either degraded or contained large lipid droplets. Melanosomes were arranged apically, but showed signs of degeneration. Some melanosomes appeared degenerate composed of noticeable empty space. Immunolabeling of H3 histone protein was positive within the nucleus and in the cytoplasm near the nucleus (Figure 4C).

The *Ccl2*$^{-/-}$/*Cx3cr1*$^{-/-}$ double-knockout mutant had severe retinal lesions. Abundant enDNA, clustered pyknotic material and fragmented nuclear envelope were identified in the cytoplasm near the nuclei (Figure 3D). In the RPE, the cytoplasmic organelles appeared highly abnormal with numerous vacuoles, lipid droplets, and large amounts of glycogen (Figure 5D). Mitochondria appeared degenerative, with poor definition of their cristae (Figure 5D). Some mitochondria also possessed large lipid droplets and contained vacuoles. There were autophagosomes (Figure 5D lower left corner). Melanosomes were scattered throughout the cell. Some melanosomes appeared disintegrated with large empty space forming in their centers. Other melanosomes appeared degenerate, with blurry edges or significant discoloration. Immunolabeling of H3 histone protein was positive within the nucleus and in the cytoplasm near the nucleus (Figure 4D).

No enDNA leakage was observed in the *vastus medialis* muscles from all four mouse strains. Nuclear membranes appeared intact without leakages (Figure 6). Clumpy material appeared in the cytoplasm of myocytes from the C56BL/6N, *Ccl2*$^{-/-}$ and *Ccl2*$^{-/-}$/*Cx3cr1*$^{-/-}$ mutant strains, but was likely glycogen or myosin (Figure 6C–D). Some mitochondria in the muscle cells of the three mouse strains with *Crb1*^{rd8} mutation also appeared mildly degenerate, with lesser degree than was observed in the RPE (Figure 7C–D).

All results are compared and summarized in Table 1.

DISCUSSION

In the literature, enDNA has no mention in the RPE. However, extrachromosomal elements (EEs) have been the focus of more research [2,3]. EEs do not bear similarities to enDNA; they differ in size, location, in having special functions, and are not associated with cellular abnormalities [2], while enDNA seems to be of random size and origin and associated with a breakage in the nuclear membrane. EEs are circular multimers of DNA, often between 500 bp and 20 kbp in size that are physically separated from the chromosomes and include episomes, minichromosomes, small polydispersed DNAs or double minutes [2,3]. Many types of EEs have been described as consistent with a predictable size range, but none have been described as existing in the cytoplasm [2]. Rearrangements that generate EEs occur randomly and non-randomly, highly-regulated, and involve specific chromosomal locations such as V(D)J-recombination, telomere maintenance mechanisms, and c-myc deregulation [2]. The only EEs that might be found in the cytosol are those of leaked mtDNA, but even then it would appear only under catastrophic circumstances [8].

Despite the systemic nature of the *Crb1*^{rd8} mutations in the mice that we examined, enDNA leakage was only found in ocular but not non-ocular (muscular) cells. This suggests that the nuclear DNA leakage is a phenomenon unique to the affected tissue or organ. Furthermore, the lack of apoptotic signs in the RPE cells, as well as the generally unhealthy appearance of

cells with enDNA, support our hypothesis that enDNA does not appear in the normal cell cycle or during apoptosis.

The fact that enDNA leakage can be seen in a 90-nm-thick section is indicative that the leakage may be taking place on the entire nuclear membrane and the cell could be undergoing catastrophic chromatin or nuclear membrane disintegration. Although chromatin elimination could actually be part of a differentiation process, which requires the unloading of DNA, this seems unlikely in the case of RPE cells since this differentiation process takes place within the nucleus and has not been described to cause enDNA leaks [2]. It is evident that enDNA emerges from the nucleus (Figure 3B–D) and is confirmed with immunolabeling using an antibody specific to the H3 histone protein which is unique to eukaryotic DNA (Figure 4B–D). Mitochondrial DNA would not possess H3 proteins, and the mice were kept in a clean environment without microorganism infection.

The uniqueness of enDNA leakage in the RPE of the three mouse strains with dysplastic and/or degenerative neural retinal lesions suggests a potentially useful role as a biomarker for retinal pathology. Thus far, we are unaware of any association between this phenomenon and retinal diseases such as AMD. If enDNA turned out to be associated with these mice having progressive retinal degeneration, then efforts to quantify abnormal cells presenting enDNA leakage, for instance, may be used to gauge the health of RPE.

Furthermore, enDNA leakage may be detected by cGAS, which could trigger an inflammatory response in the tissues [4]. The cGAS protein is known to detect cytosolic DNA, and its activation is known to produce an inflammatory immune response by INF-β through the cGAS-cGAMP signaling pathway [4]. If cytoplasmic enDNA is indeed recognized by cGAS and causing inflammation, then enDNA and the cGAS-cGAMP signaling pathway may also be a clinical target for future preventative treatments against retinal degeneration.

Although the cause of enDNA leakage remains unknown, one tentative explanation is energy-centric and attributes the phenomenon to degenerating mitochondria, which were observed in the abnormal RPE cell [9]. Mitochondrial decline is closely linked with cell health, as they provide energy for all cellular differentiation and functions [10]. Maintaining homeostasis, such as managing and organizing DNA within the nucleus, is an energy intensive operation, and enDNA leakage into the cytoplasm may be a result of the loss of homeostasis as the cell energy generation is compromised [11].

The degeneration of mitochondria in the cell may be caused by hypoxia. AMD is reported to associate with hypoxia and the activity of HIF-1 [12]. Vacuolization and excessive glycogen observed in abnormal RPE cells (Figures 3 and 5) are suggestive of an advanced state of autophagy induced by the mitochondria under hypoxic conditions [13]. This hypoxic breakdown may continue until mitochondria lose function, leading to the buildup of cytoplasmic glycogen due to switching from oxidative phosphorylation to glycolysis to generate energy. Glycogen is a common target of autophagy, and it has been suggested that variability of glycogen content is associated with mitochondrial activity [14,15]. That an abundance of glycogen is present within the cytoplasm lends credibility to the idea that

mitochondria may have lost function, leading to the cell-wide loss of homeostasis, which in turn could lead to the leakage of enDNA into the cytoplasm, inducing INF-β signaling and triggering an inflammatory response, which was not visible in our study. However, if enDNA precedes mitochondrial damage, then the subsequent inflammatory response causes the damage.

The observation that degeneration in the muscles of the three strains with *Crb1*^{rd8} mutation is much less extensive than in the RPE, might be explained by differential effect of hypoxia on the two tissues. Skeletal muscles, such as the *vastus medialis*, are frequently exposed to a hypoxic environment during physical exertion, and as such are resilient to hypoxia-induced damage [16]. Skeletal muscle has also been shown to readily adapt to long-term exposure to hypoxic environments by reducing total mitochondrial content of myocytes [17]. RPE cells, by comparison, are less tolerant to hypoxia, which may explain the differential expression of the damage between the two tissues [18].

In conclusion, our ultrastructural observations coupled with EM immunolabeling have shown that chromatin fragmentation and leakage into the cytoplasm appear to be an RPE-specific phenomenon, within the context of our survey, which seems to be energy-related since it is associated with mitochondrial aberrations. RPE malfunction, especially in AMD, may have an immunological component, and since enDNA is known to trigger the release of interferon, enDNA could be the culprit in the initiation of the inflammatory process that leads to the devastation of the tissue [4,19,20]. Further work is required to elucidate the enDNA phenomenon and the feasibility of its utility for early clinical detection of AMD in humans.

References

1. Maeda T, Chijiiwa Y, Tsuji H, et al. Somatic DNA recombination yielding circular DNA and deletion of a genomic region in embryonic brain. Biochem Biophys Res Commun. 2004; 319:1117–23. [PubMed: 15194483]
2. Kuttler F, Mai S. Formation of non-random extrachromosomal elements during development, differentiation and oncogenesis. Semin Cancer Biol. 2007; 17:56–64. [PubMed: 17116402]
3. Cohen S, Segal D. Extrachromosomal circular DNA in eukaryotes: Possible involvement in the plasticity of tandem repeats. Cytogenet Genome Res. 2009; 124:327–38. [PubMed: 19556784]
4. Li XD, Wu J, Gao D, et al. Pivotal roles of cGAS-cGAMP signaling in antiviral defense and immune adjuvant effects. Science. 2013; 341:1390–94. [PubMed: 23989956]
5. Tuo J, Bojanowski CM, Zhou M, et al. Murine ccl2/cx3cr1 deficiency results in retinal lesions mimicking human age-related macular degeneration. Investig Ophthalmol Vis Sci. 2007; 48:3827–36. [PubMed: 17652758]
6. Mattapallil MJ, Wawrousek EF, Chan CC, et al. The Rd8 mutation of the Crb1 gene is present in vendor lines of C57BL/6N mice and embryonic stem cells, and confounds ocular induced mutant phenotypes. Investig Ophthalmol Vis Sci. 2012; 53:2921–7. [PubMed: 22447858]
7. Chu XK, Wang Y, Ardeljan D, et al. Controversial view of a genetically altered mouse model of focal retinal degeneration. Bioengineered. 2013; 4:130–5. [PubMed: 23196746]
8. Shimada K, Crother TR, Karlin J, et al. Oxidized mitochondrial DNA activates the NLRP3 inflammasome during apoptosis. Immunity. 2012; 36:401–14. [PubMed: 22342844]
9. Cogliati S, Frezza C, Soriano ME, et al. Mitochondrial cristae shape determines respiratory chain supercomplexes assembly and respiratory efficiency. Cell. 2013; 155:160–71. [PubMed: 24055366]

10. Karunadharma PP, Nordgaard CL, Olsen TW, Ferrington DA. Mitochondrial DNA damage as a potential mechanism for age-related macular degeneration. Investig Ophthalmol Vis Sci. 2010; 51:5470–9. [PubMed: 20505194]
11. Kotiadis VN, Duchen MR, Osellame LD. Mitochondrial quality control and communications with the nucleus are important in maintaining mitochondrial function and cell health. Biochim Biophys Acta. 2014; 1840:1254–65. [PubMed: 24211250]
12. Arjamaa O, Nikinmaa M, Salminen A, Kaarniranta K. Regulatory role of HIF-1alpha in the pathogenesis of age-related macular degeneration (AMD). Ageing Res Rev. 2009; 8:349–58. [PubMed: 19589398]
13. Zhang H, Bosch-Marce M, Shimoda LA, et al. Mitochondrial autophagy is an HIF-1-dependent adaptive metabolic response to hypoxia. J Biol Chem. 2008; 283:10892–903. [PubMed: 18281291]
14. Kotoulas OB, Kalamidas SA, Kondomerkos DJ. Glycogen autophagy in glucose homeostasis. Pathol Res Pract. 2006; 202:631–8. [PubMed: 16781826]
15. DiMauro S, Schotland DL, Bonilla E, et al. Progressive ophthalmoplegia, glycogen storage, and abnormal mitochondria. Arch Neurol. 1973; 29:170–9. [PubMed: 4273246]
16. Gawlitta D, Li W, Oomens CW, et al. The relative contributions of compression and hypoxia to development of muscle tissue damage: An in vitro study. Ann Biomed Eng. 2007; 35:273–84. [PubMed: 17136445]
17. Hoppeler H, Vogt M, Weibel ER, Fluck M. Response of skeletal muscle mitochondria to hypoxia. Exp Physiol. 2003; 88:109–19. [PubMed: 12525860]
18. Castillo M, Bellot JL, Garcia-Cabanes C, et al. Effects of hypoxia on retinal pigmented epithelium cells: Protection by antioxidants. Ophthal Res. 2002; 34:338–42.
19. Ardeljan D, Chan CC. Aging is not a disease: Distinguishing age-related macular degeneration from aging. Progr Retin Eye Res. 2013; 37:68–89.
20. Ardeljan, D.; Wang, Y.; Shen, DF., et al. Treatment with recombinant interleukin-17A reduces ARPE-19 cell viability. Paper presented at: ARVO; 2012; Fort Lauderdale, FL.

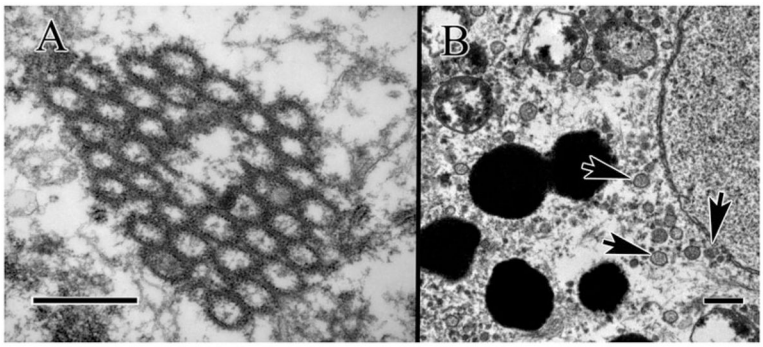

FIGURE 1.

Extranuclear DNA (enDNA) from clinical specimen of advanced AMD cases. (A) Circular strands of pyknotic chromatin clumping together within the cytoplasm, (B) enDNA emerging from nucleus (lower right arrow), and circularized (two left arrows). Scale bar = 500 nm.

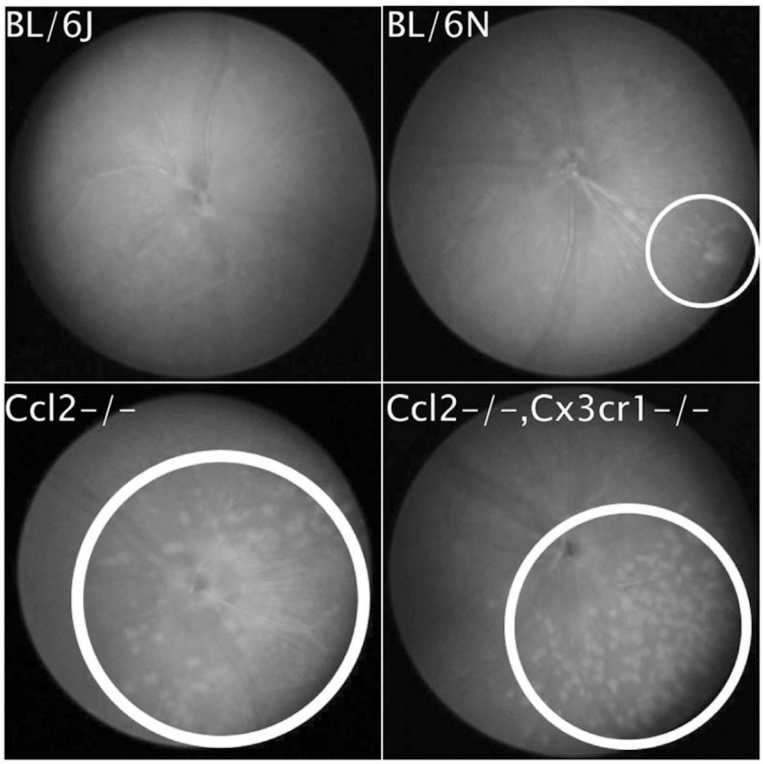

FIGURE 2.

Retinal fundoscopy results for each mouse strain (all OS). Retinal lesions in each eye are circled. (A) The wild-type BL/6J strain, (B) the BL/6N strain, (C) the $Ccl2^{-/-}$ knockout mutant, and D) the $Ccl2^{-/-}/Cx3cr1^{-/-}$ double-knockout mutant.

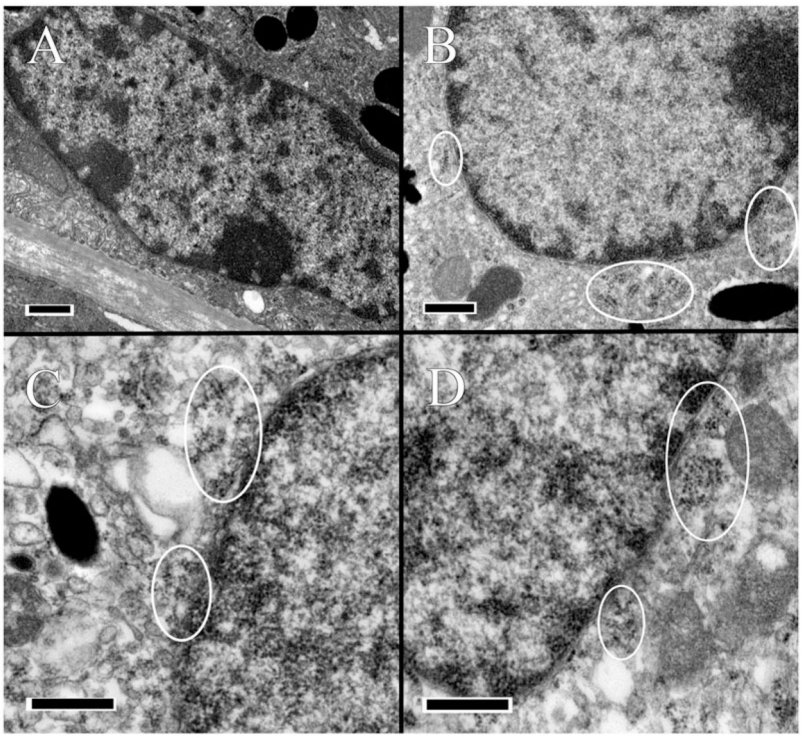

FIGURE 3.

Ultrastructural analysis of RPE. Suspected enDNA leakage is circled. (A) The wild-type BL/6J strain appears normal and healthy. (B) In the BL/6N strain, the nuclear envelop appears porous, with pyknotic material present in the cytoplasm. The cytoplasm is irregular with some vacuolization, and mitochondria appear unhealthy with poor definition of their cristae. (C) In the *Ccl2*$^{-/-}$ knockout mutant, the nuclear envelop is highly irregular, with pyknotic material leaking out into the cytoplasm. The cytoplasm appears abnormal with some tiny vacuolization. (D) In the *Ccl2*$^{-/-}$, *Cx3cr1*$^{-/-}$ double-knockout mutant, the nuclear envelop appears irregular with pyknotic material present in the cytoplasm, which is abnormal, with a high degree of vacuolization, and the mitochondria appear abnormal with poorly-defined cristae. Scale bar = 500 nm.

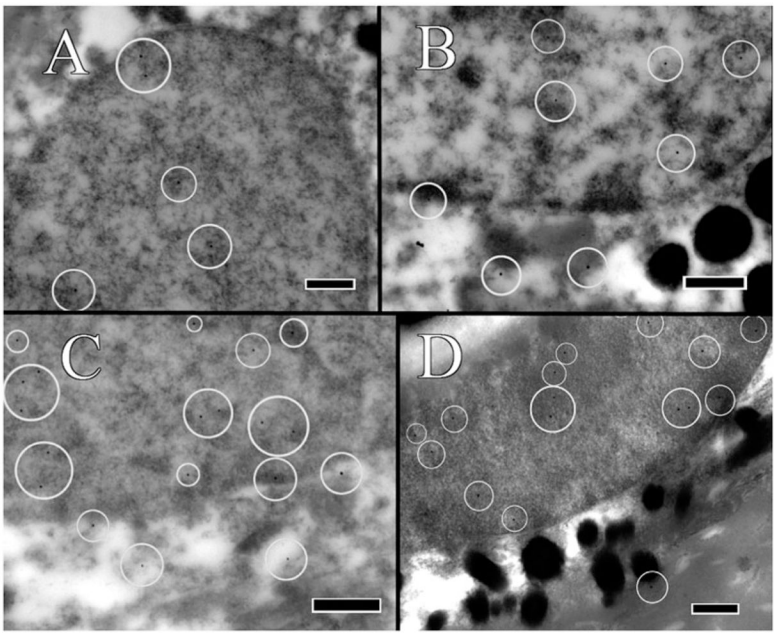

FIGURE 4.

RPE immunolabeled with rabbit-anti-mouse H3 polyclonal antibody. Gold-conjugated protein A secondary antibody is 20 nm in size, and have been circled for ease of identification. (A) Labeling in the C57/BL6J mouse is only within the nucleus. (B) Labeling in the C57/BL6N mouse occurs within both the nucleus and the cytoplasm. (C) Labeling in the *Ccl2*$^{-/-}$ knockout mutant occurs within both the nucleus and the cytoplasm. (D) Labeling in the *Ccl2*$^{-/-}$/*Cx3cr1*$^{-/-}$ double-knockout mutant occurs in both the nucleus and the cytoplasm. A lack of strong signaling might be attributed to the advanced state of degeneration within the cell. Scale bar = 500 nm.

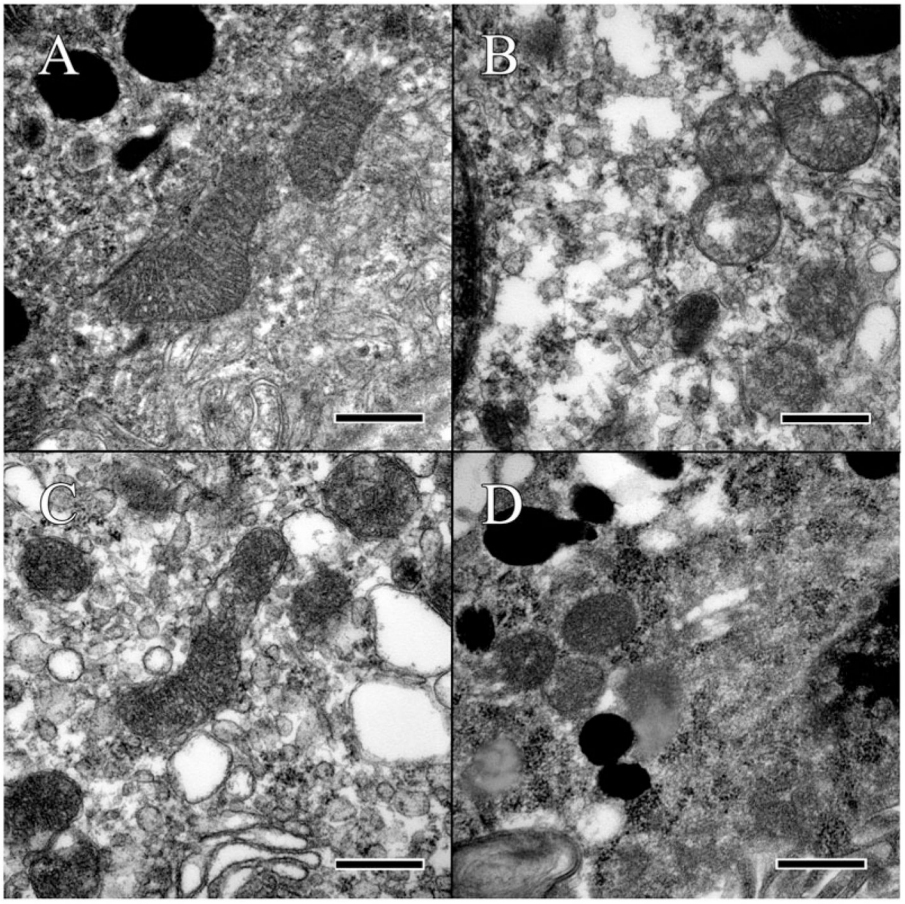

FIGURE 5.

Analysis of mitochondria in the RPE. (A) Mitochondria of the wild-type C57BL/6J strain presented with well-defined cristae and membranes. Some glycogen or other protein artifacts can be seen within the mitochondria and surrounding cytoplasm. (B) Mitochondria in the C57BL/6N appear abnormal, with ill-defined cristae and the formation of lipid vacuoles within the mitochondrial. (C) Mitochondria of the Ccl2 knockout lack definition of the cristae and are surrounded by vacuoles. (D) Mitochondria of the double knockout are surrounded by glycogen and have lost all definition of their inner membrane, as well as the sharpness of the outer membrane. Scale bar = 500 nm.

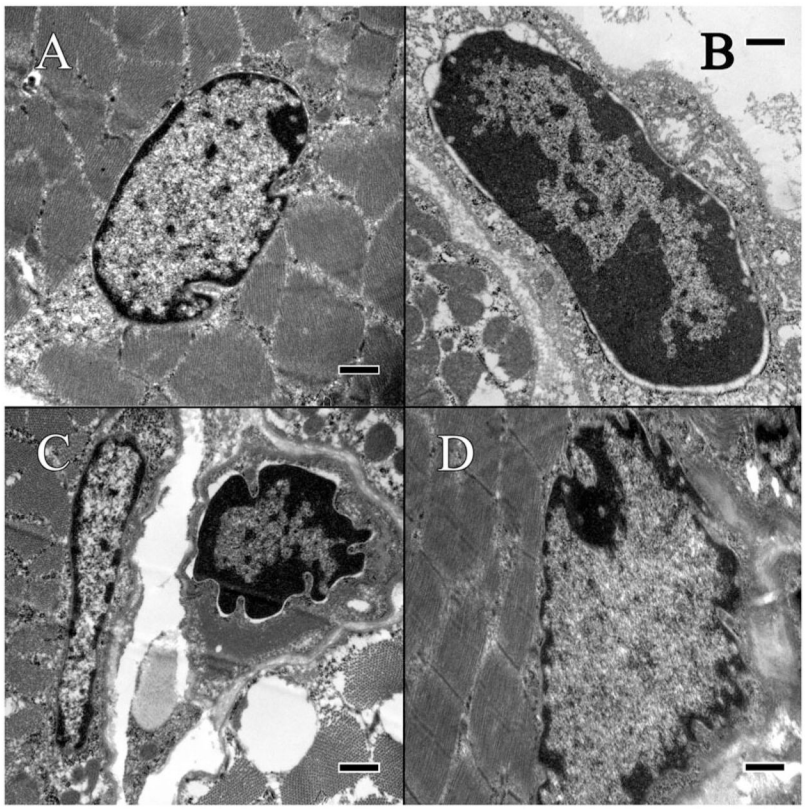

FIGURE 6.

Ultrastructural analysis of *vastus medialis* muscle in mouse strains. (A) The wild-type C57BL/6J mouse appears mostly normal and healthy, with some normal glycogen aggregation within the cytoplasm. (B) The C57/BL6N strain appears in distress, with cytoplasm pulling back from the nuclear envelop, which remains unbroken. Glycogen can be noted aggregating along the edge of the cytoplasm where the nuclear envelop has separated. (C) The *Ccl2*$^{-/-}$ strain appears somewhat degenerate, with lipid and glycogen accumulation noticeable within the muscle fiber. The nuclear envelop remains intact, and there is no sign of enDNA leakage. (D) The *Ccl2*$^{-/-}$/*Cx3cr1*$^{-/-}$ strain lacks strong definition of the nuclear envelop. Scale bar = 500 nm.

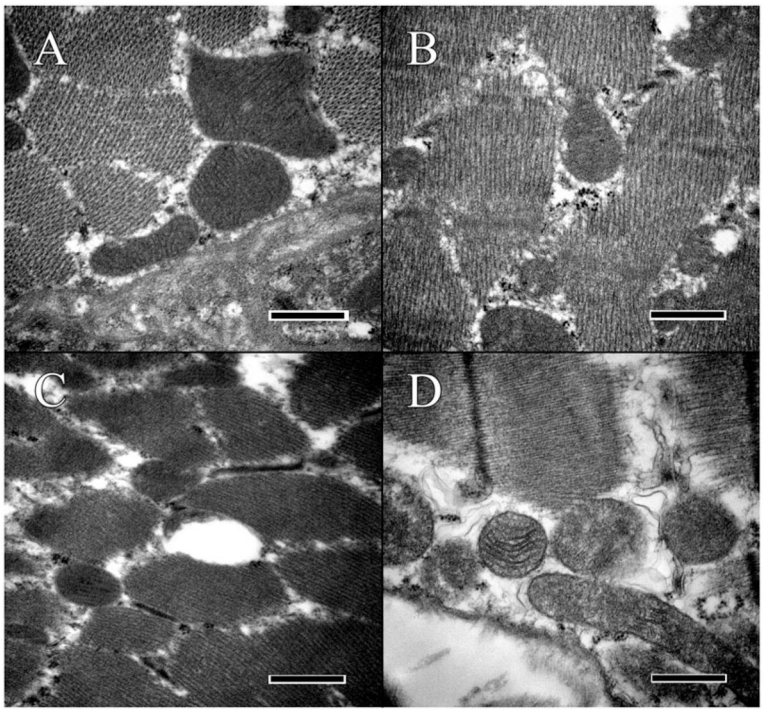

FIGURE 7.

Analysis of mitochondria in *vastus medialis* muscle. (A) Mitochondria of the C57BL/6J mouse appear normal, with defined cristae. Some glycogen is present. (B) The mitochondria of the C57BL/6N mouse appear distressed, lacking well-defined cristae. More glycogen can be observed as compared to the BL/6J strain. (C) Mitochondria in the *Ccl2*$^{-/-}$ knockout mutant appear distressed, with no definition of the cristae. Significant amounts of glycogen can be observed within the myocyte. (D) Mitochondria of the *Ccl2*$^{-/-}$/*Cx3cr1*$^{-/-}$ double-knockout mutant appear highly degenerate, with both loss of definition within the cristae and loss of the outer membrane. Significant amounts of glycogen can be observed within the myocyte. Scale bar = 500 nm.

TABLE 1

Summary of results by tissue.

	Tissue characteristics							
	RPE				Muscle: *vastus medialis*			
Mouse strain	**enDNA**	**Mitochondrial Degeneration**	**Autophagosome**	**Glycogen**	**enDNA**	**Mitochondrial Degeneration**	**Autophagosome**	**Glycogen**
C57/BL6J	−	−	−	+	−	−	−	+
C57/BL6N	+	+	−	++	−	+	−	+
Ccl2$^{-/-}$	+	++	−	++	−	+	−	+
Ccl2$^{-/-}$/*Cx3cr1*$^{-/-}$	+	++	+	+++	−	+	−	+

Note: − = lacking, + = present at normal quantity, ++ = moderately elevated, +++ = highly elevated.